CJC Chinese Journal of Chemistry 中国化学 · An International Journal

For submission: https://mc.manuscriptcentral.com/cjoc
For published articles: https://onlinelibrary.wiley.com/journal/16147065

Concise Report

Cite this paper: *Chin. J. Chem.* **2022**, *40*, 2927—2932. **DOI: 10.1002/cjoc.202200481**

Organic Solar Cells at Stratospheric Condition for High Altitude Platform Station Application†

Ram Datt,[a] Harrison Ka Hin Lee,*[,a,b] Guichuan Zhang,[c,d] Hin-Lap Yip,*[,d,e,f,g] and Wing Chung Tsoi*[,a]

[a] *SPECIFIC, Faculty of Science and Engineering, Swansea University, Bay Campus, Fabian Way, Swansea, SA1 8EN, United Kingdom*
[b] *Department of Physics, City University of Hong Kong, Kowloon, Hong Kong SAR, China*
[c] *School of Semiconductor Science and Technology, South China Normal University, Foshan, Guangdong 528225, China*
[d] *State Key Laboratory of Luminescent Materials and Devices, South China University of Technology, 381 Wushan Road, Guangzhou, Guangdong 510640, China*
[e] *Department of Materials Science and Engineering, City University of Hong Kong, Kowloon, Hong Kong, China*
[f] *School of Energy and Environment, City University of Hong Kong, Kowloon, Hong Kong, China*
[g] *Hong Kong Institute for Clean Energy, City University of Hong Kong, Kowloon, Hong Kong, China*

Comprehensive Summary

High specific power or power to mass ratio is a critical concern of photovoltaic (PV) for aerospace applications. Organic solar cells (OSCs) have advantages such as high absorption coefficient, compatibility with flexible substrate, light-weight, *etc*. Moreover, recently OSCs achieved power conversion efficiency (PCE) over 20% with the incorporation of the non-fullerene based small molecule acceptor and high specific power is believed to be obtained. To enter the market, high-altitude platform station (HAPS) is perhaps the first place to start with. In this work, we explore and compare the in-situ performance of two high performing OSCs, using the same donor but different acceptors, in mimic HAPS environment where the pressure, temperature and the illumination conditions are controlled. We found that the use of acceptor can result in substantial difference in the performance at low temperatures.

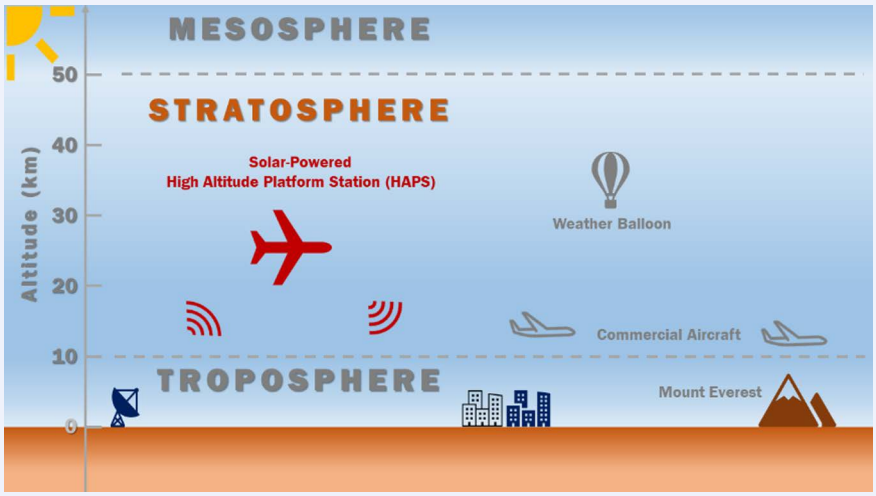

Keywords

Organic solar cells | Stratosphere | High-altitude platform station | Low-temperature physics | Donor-acceptor systems

*E-mail: kahinlee2@cityu.edu.hk, a.yip@cityu.edu.hk, w.c.tsoi@swansea.ac.uk
† Dedicated to the Special Issue of Emerging Investigators in 2022.

View HTML Article | Supporting Information

Background and Originality Content

Organic solar cells (OSCs) are an attractive class of photovoltaics, and they require carbon-based organic molecules to absorb the light and generate the charge carriers.[1-3] The key advantages of OSCs are easy optical and electronic properties tunability of organic molecules, low cost, low temperature process, roll to roll processability, compatibility with flexible substrates, requiring non-toxic raw materials, and having versatile applications such as transparent, indoor, agrivoltaics and aerospace.[4-9] The aerospace industry is growing progressively and there is a high requirement of cost-effective and low weight solar cells in near future. In aerospace, the operating unmanned vehicle in the stratosphere is attaining interest for communication, disaster management, defence, and surveillance, and the operating region is called HAPS. The HAPS is usually an unmanned aircraft systems (UAS) flying at 20—25 km above earth surface, within the stratosphere of the atmosphere, as illustrated in the comprehensive graphic. The duration of the mission could be as short as few months, few weeks or even one-off mission, depending on the aim. Zephyr, an UAS developed by Airbus Ltd., can provide a range of continuous surveillance, and help in detection of environmental conditions. It relies on solar energy with batteries charged in the daytime to provide power to flight in the night-time. To decide the choice of solar cells, it is essential to have high performance as well as light weight, *i.e.*, called high specific power. It maximizes the energy generation; meanwhile keeps the minimal energy consumption due to the weight of the solar modules. Besides, the solar cells must withstand the HAPS environmental condition, which includes high temperature variation (–20 to 10 °C on average daytime, and up to –85 °C in night-time), ultra-violet (UV) rich solar radiations (AM0, 1366.1 W/m^2), and low pressure (1 to 250 mbar).[10] Inorganic solar cells have been well studied for aerospace application. Their costly fabrication process and low specific power restrict their use for other application purposes. On the other side, the OSCs are well-known for their light weight and highly flexible nature.[11] Traditional silicon-based solar cells are costly, heavy, non-flexible, and has a specific power of ~0.38 W/g.[12] Inorganic multijunction solar cells suffered from thick active and rigid structure and delivered specific power of ~0.4—0.8 W/g and could reach up to 3.8W/g after proper engineering of metal contact.[12] In the last decade, organic-inorganic perovskite solar cells demonstrated a comparable PCE to inorganic solar cells and it is a low cost-solution processable solar technology and showed specific power of 23 W/g.[13] The perovskite solar cells also are potential candidates for HAPS application.[10] Whereas, the OSCs demonstrated high specific power of 10—14 W/g.[11,14-15] Although these specific powers were calculated for the low PCE OSCs system, it is expected to get high specific power for the recently developed devices. Besides, high specific power, the low-cost and roll to roll fabrication of OSCs appeal revolutionary for space industry. Thanks to development of non-fullerene-based small molecule acceptors (NFA), as it has led to PCE up to 19.3% for single junction and 20.2% for tandem structure OSCs under AM 1.5G.[16-22] It is believed that higher specific power can be achieved as long as the state-of-the-art OSCs systems are used with those extra-light weight device architectures. Although the absolute performance of OSCs is not among the best, it has high potential of having a high specific power device which coordinates well with the application for HAPS or even space usage. Schreurs *et al.*[23] studied the OSCs by sending devices with stratospheric balloon flight under the optical sensors based on CARbon-materials (OSCAR) project. The devices were made of PBDTTPD:$PC_{71}BM$ and PCPDTQx(2F):$PC_{71}BM$ photoactive layer. Reb *et al.*[24] reported the HOPVs (Hybrid perovskite and organic photovoltaics) devices investigation during a suborbital rocket flight. The devices used in this study were PBDB-T:ITIC and PTB7-Th:$PC_{71}BM$ based OSCs systems. Furthermore, the numerous polymer active layer system such as P3HT:PCBM, PTB7-Th:$PC_{71}BM$, PCDTBT:$PC_{71}BM$, PBDB-T:ITIC, BTR:$PC_{71}BM$, *etc.* have been studied under various environmental conditions including operating temperature, radiation stability, and thermal cycling, and these OSCs delivered the promising outcomes.[14,25-30] Under proton radiation (1012 p cm^{-2}), OSCs showed more robustness than the currently dominating solar cells such as the GaAs/III–V semiconductor photovoltaic for space application.

In this work, we explore the feasibility of using state-of-the-art OSCs for HAPS applications. A benchmark OSCs system, the PM6:Y6 was tested in a mimic HAPS condition in which the temperature ranges were from –20 °C to 10 °C under a pressure of 10 mbar. However, we extended the measuring temperature to 80 °C or even –100 °C as a check to ensure that the OSCs devices are not degraded due to low temperature. Also, it is interesting to understand how these benchmark devices would perform under wide temperature (–100 °C to 80 °C) range as it is possible to transfer the OSCs from HAPS to space application, which has a much broader temperature coverage. Regarding the solar spectrum, since the sun light is expected to be collected within the stratosphere, and that is more similar to AM0 spectrum when compared to the standard AM1.5G spectrum, therefore, AM0 spectrum was used in this study. We also tested another device system by changing the electron acceptor (Y6) to IT-4F.[31] Despite decent performance at room temperature, and at low temperature, the PCE of PM6:IT-4F devices dropped substantially when compared to the PM6:Y6 system. The molecular structures of PM6, Y6, and IT-4F are shown in Scheme 1.

Scheme 1 Chemical structures of PM6, Y6, and IT-4F organic molecules

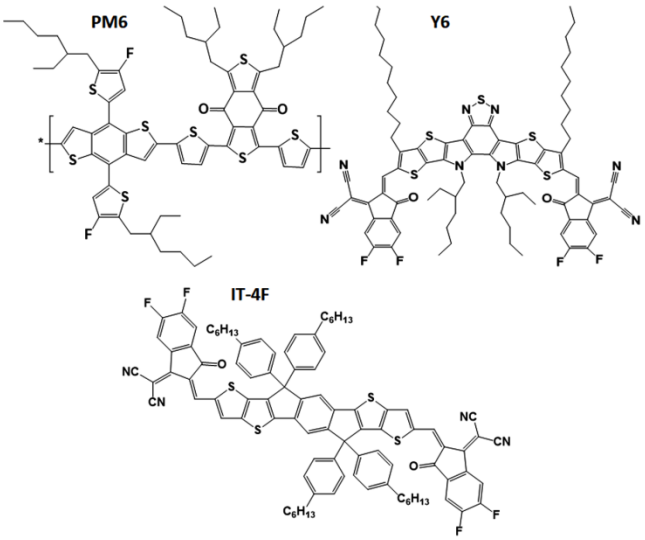

Results and Discussion

Photovoltaic performance

The PM6:Y6 devices were examined under the standard testing condition AM1.5G, and the external quantum efficiency (EQE) were also measured to confirm the short-circuit current density (J_{sc}) under both AM1.5G and AM0 irradiations. Figure 1(a) shows the EQE spectrum of the PM6:Y6 device, along with the AM1.5G and AM0 spectra. For the AM0 spectrum, since it does not possess the absorption features due to the atmosphere, it has broader UV coverage of down to 200 nm, a smoother spectrum in the near-infrared region, and an overall higher intensity of 136.6

mW/cm^2 while 100 mW/cm^2 for AM1.5G. To achieve AM0 spectrum, an AM0 filter was used instead of an AM1.5G filter, and the light intensity was calibrated by using calculated J_{EQE} value of OSCs devices under AM0 irradiation. Figure 1b shows the AM1.5G and AM0 room temperature current density-voltage (*J-V*) characteristics of the PM6:Y6 device, and the corresponding PCE are 15.9% and 13.6%. As expected, there is a drop in PCE under AM0, which is 0.86x of the PCE under AM1.5G, mainly due to the compositional difference of the two spectra. The ratio of this PCE is similar to the ratio obtained by other PV technologies, such as 0.86x for GaAs and 0.92x for perovskite solar cells.[10] With the higher intensity under AM0, the J_{SC} was increased from 25.60 to 30.6 mA/cm^2, and fill factor (FF) decreased from 73.16% to 71.68 %, while the open-circuit voltage (V_{oc}) remained similar. The difference between J_{sc} calculated from *J-V* and EQE was under 4%. The EQE spectra of PM6:Y6 system OSCs are shown in Figures S1 and S2 (Supporting Information) under AM0 and AM1.5 G irradiations, respectively.

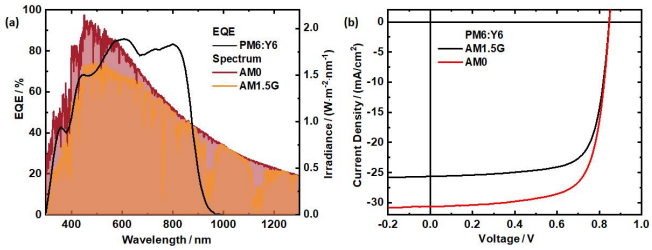

Figure 1 (a) Spectra of AM0, AM1.5G and the EQE of the PM6:Y6 OSCs. (b) *J*-V characteristics of PM6:Y6 OSCs under AM0 and AM1.5G illumination.

Temperature dependent performance under AM0

The solar cells operating performance highly depends on the environment. The temperature within the stratosphere depends on the altitude, latitude, day-and-night alternation, *etc*. Typically, for HAPS application, temperature ranges from −85 °C to 10 °C. During the daytime, the solar cell temperature is between −20 °C and 10 °C. Although the actual operating temperature range is not too large, the solar cells still experience low temperatures (as low as −85 °C) during the night-time. As a comparison, we also fabricated another OSCs system, PM6:IT-4F, the same polymer donor blended with a well-functioning NFA (IT-4F). Figure 2 shows the *J-V* curves at different temperatures of both the systems and the changes in the device parameters are summarized in Figure 3. Similar behaviour in J_{sc} was observed for both the systems when the temperature was above *c.a*. −20 °C. Whereas, when the temperature was lowered, both the systems showed decrease in J_{sc} while the decrease in the PM6:IT-4F device is more pronounced. For the PM6:Y6 system, its J_{sc} can retain 95% of the room temperature value at *c.a*. −50 °C. In terms of the V_{oc}, both the systems showed a very similar trend in which the V_{oc} decreases with increasing temperature and vice-versa. This phenomenon is attributed to temperature-dependent mobility.[32-36] At temperatures above −20 °C, the temperature-dependence is quite linear. However, at a temperature below −20 °C, the linear dependence starts to deviate from the linear trend which is observed elsewhere.[37-40] For the FF, the PM6:Y6 device shows a very stable behaviour at a temperature above −10 °C, a variation of less than 1% when compared to the room temperature value. On the other hand, for the temperature above 0 °C, the PM6:IT-4F device shows a slightly positive temperature dependence of the FF. At lower temperatures, the FF of both systems drops significantly with a more pronounced drop for PM6:IT-4F. Overall, combining the effect of temperature on the three PV parameters, the PCE of PM6:Y6 and PM6:IT-4F show a peak at 20 °C temperature. Within the range of *c.a*. ±20 °C around the temperature of the PCE peak, both the systems show a fairly stable PCE trend against temperature. Comparing the two systems studied here, PM6:Y6 is clearly a more suitable system as it has a stable PCE within the temperature range of operation, −20 °C to 10 °C. The Y6 and IT-4F molecules have different molecular packing, which can influence the charge transport properties, and directly impact the device performance.[41] Furthermore, the Y6 molecule forms a less amorphous film than the IT-4F molecule and influences the OSCs performance.[41-42] These could be a reason to deliver better performance of PM6: Y6 than PM6: IT-4F.

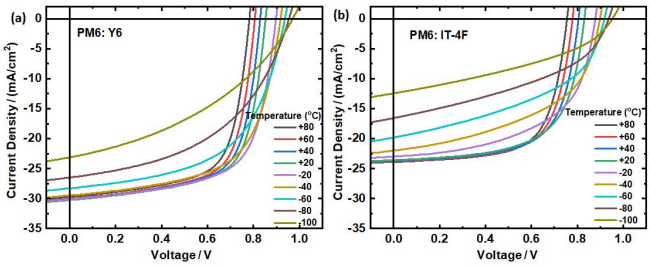

Figure 2 *J-V* characteristics of (a) PM6:Y6, and (b) PM6:IT-4F OSCs at different temperatures range from −100 °C to 80 °C under AM0 solar irradiation.

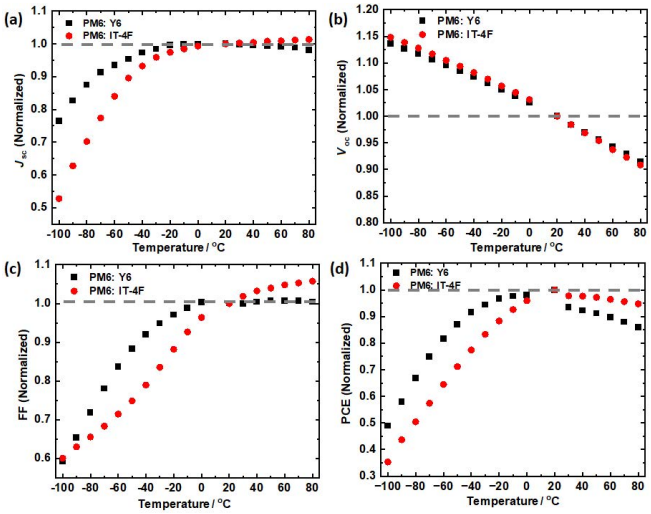

Figure 3 The comparison of device parameters (a) J_{sc}, (b) V_{oc}, (c) FF, and (d) PCE for both the systems, measured under 80 to −100 °C temperature. Data are normalized to the values at 20 °C.

Intensity dependent measurements

The light-intensity dependence measurements of the photovoltaic performance of both PM6:Y6 and PM6:IT-4F systems were studied systematically. A series of neutral density filters were used to achieve different light intensity under AM0. The diode ideality factor (n) and recombination parameters (α) were calculated according to $V_{oc} \propto nkT/q \ \ln P_{light}$ and following the relationship of $J_{sc} \propto P_{light}^{\alpha}$, respectively,[43-44] where α, q, T, k, and P_{light} are recombination parameter, elementary charge, absolute temperature, Boltzmann constant, and incident light intensity, respectively. The value of n reflects the charge carrier recombination in the devices. If n deviates from the ideal value 1 and approaches 2, it implies domination of trap-assisted recombination.[46] For $n < 1$, it may imply surface recombination.[45-46] The α close to unity shows weak biomolecular recombination under short circuit conditions. These two parameters (n and α) were calculated for both systems

under three different temperature conditions (80, 20, and –100 °C). Figure (4a) and Figure (4b) show the V_{oc} vs. light intensity plots for PM6:Y6 and PM6:IT-4F based devices, respectively. The smaller n of PM6:Y6 compared to those of PM6:IT-4F device at the corresponding temperatures indicates that trap-assisted recombination is more suppressed in PM6:Y6 system.[47-48] At 20 °C, the PM6:Y6 and PM6:IT-4F systems have a slope of 1.30kT/q and 1.46kT/q, respectively. Whereas, at higher temperatures (80 °C) the slopes were increased to 1.35kT/q and 1.50kT/q for PM6:Y6 and PM6:IT-4F, respectively. It indicated an increase in the trap-assisted recombination at higher temperatures and caused additional V_{oc} loss. Whereas, at a lower temperature (–100 °C) the slopes were 1.13kT/q and 1.11kT/q of PM6:Y6 and PM6:IT-4F devices and a decrease in the slope was observed for both systems compared to room and high-temperature measurements. It shows a decrease in trap-assisted recombination, and an improvement in open-circuit voltage at low temperature. Figures (4c) and (4d) show the log-log plot of J_{sc} vs. light intensity measurement of PM6:Y6 and PM6:IT-4F blend system-based devices. The values of α were calculated to be 0.9994 (80 °C), 0.9989 (20 °C), and 0.9127 (–100 °C) for PM6:Y6 devices. Whereas, for PM6:IT-4F device the α values were 0.9802, 0.9832, and 0.7775 at 80 °C, 20 °C, and –100 °C, respectively. At low (–100 °C) temperatures, both systems suffered from more significant biomolecular recombination losses. Whereas PM6:Y6 system has a low deviation of α value from its unity as compared to PM6:IT-4F and shows lower biomolecular recombination in PM6:Y6 device under low-temperature measurement. The high drop in J_{sc} (Figure 3a) of PM6:IT-4F device as compared to PM6:Y6 under low-temperature measurement, supports the lower α value of PM6:IT-4F than that of the PM6:Y6 system.[49]

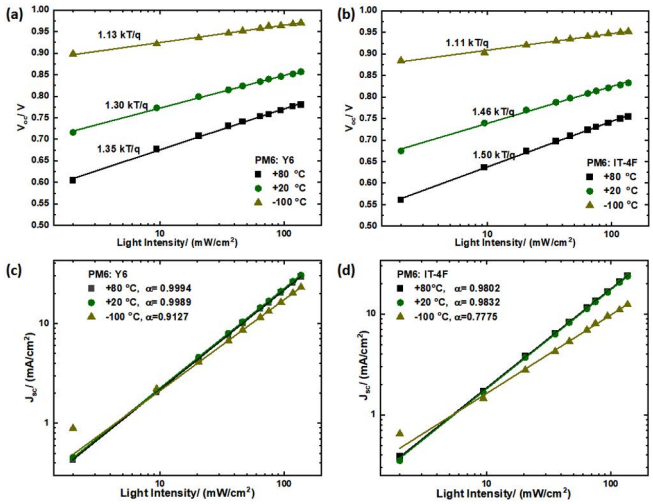

Figure 4 The light intensity dependent measurements: (a) V_{oc} vs. intensity, (c) J_{sc} vs. intensity of PM6:Y6 device. (b) V_{oc} vs. intensity, (d) J_{sc} vs. intensity of PM6:IT-4F device.

In outcome, the HAPS environment temperature condition was examined in benchmark OSC system, PM6:Y6, between 80 °C and –100 °C. The device performance reduction was observed under low temperature. The PCE dropped up to ~34% at –80 °C compared to that at 20 °C under AM0 solar irradiation. Moreover, for comparison the PM6:IT-4F system also was examined under the same condition and the drop in PCE for it was 50% at –80 °C. However, the PM6:IT-4F devices showed ~16% higher drop in PCE than PM6:Y6 at –80 °C as compared to the performance at 20 °C. Moreover, for the PM6:IT-4F system, PCE also dropped at high temperature compared to PM6:Y6. The PM6:Y6 is a good system for HAPS and more likely to explore for space application as it holds PCE up to 50% at –100 °C. The temperature range at lunar surface is –50 to 75 °C, as suggested by recent thermal modelling, it indicates that OSCs could be a potential choice as PM6:Y6 device's PCE dropped only 13% in that temperature region from 20 °C device performance.[50]

Conclusions

In this study, we have selected the PM6:Y6 blend system based OSCs and studied its photovoltaic performance under a broad range of temperatures according to HAPS environment conditions. Moreover, we also replaced the Y6 non-fullerene acceptor with IT-4F and examined the device's performance under similar conditions. It is found that PM6:Y6 device performed well, and the PCE dropped between –20 to 10 °C is negligible. Whereas, for PM6:IT-4F device, the PCE dropped almost 12% at –20 °C compared to its peak value. However, at –80 °C the PM6:Y6 device could still hold up to 66% of its initial value (at 20 °C). The major drops came into J_{sc} and FF under the low temperature of PM6:IT-4F device. The recombination mechanism was studied under three different temperatures: 80, 20, and –100 °C. The lower slope (kT/q) of both devices at low-temperature measurement shows a reduction in trap-assisted recombination. Whereas PM6:IT-4F device shows high bimolecular recombination as calculated value α has a large deviation from unity at –100 °C, which caused a high drop in J_{sc} compared to PM6:Y6 device. To conclude, the PM6:Y6 device performed well and showed promising performance to HAPS temperature environmental conditions. This work provides an in-strength study on a benchmark OSC system PM6:Y6 and highlights its great potential for HAPS or even space applications.

Experimental

Materials and characterization

In materials, PBDB-T-2F (PM6) (M_n = 37.0 kDa, M_w = 101.6 kDa, PDI = 2.74) was purchased from Solarmer Inc (China), IT-4F and Y6 were purchased from Derthon Optoelectronic Materials Science Technology Co., Ltd. (China), and C60-SAM was purchased from 1-Material Inc. The photovoltaic performance measurement was conducted by using Keithley 2400 and class AAA solar simulator (Newport, Model No: 94023A). The AM1.5 G irradiation was calibrated by using standard silicon solar cells. The AM0 filter was placed for creating the HAPS solar irradiation conditions. The EQE graph was measured by using QE X10 (PV measurement) system. The HAPS environment conditions were created by using a closed chamber (Linkam Scientific) as shown in Figure S3 (Supporting Information). The temperatures were controlled between 80 to –100 °C by using the liquid nitrogen and the chamber pressure was maintained at 10 mbar.

Device fabrication

The indium doped tin oxide (ITO) glass substrates were cleaned sequentially under sonication with acetone, detergent, deionized water, and isopropyl alcohol and then dried at 60 °C in a baking oven overnight, followed by a 4-min oxygen plasma treatment. Then, zinc oxide (ZnO) electron transport layer (a thickness of ~30 nm) was prepared by spin-coating at 5000 r/min for 30 s from a ZnO precursor solution (diethyl zinc, 1.5 mol/L solution in toluene, diluted in tetrahydrofuran) on ITO substrates, followed by thermal annealing at 150 °C for 30 min. A C60-SAM monolayer was prepared by spin-coating C60-SAM solution (1 mg/mL, chlorobenzene (CB) : tetrahydrofuran (THF) = 2 : 1 by volume) at 4000 r/min for 30 s, following thermal annealing at 100 °C for 5 min and then washed by CB : THF (2 : 1 by volume) solvent. The solutions of PM6:Y6 (weight ratio = 1 : 1.2) and

PM6:IT-4F (weight ratio = 1 : 1) were prepared in chloroform (0.5% 1-chloronaphthalene) and chlorobenzene (0.5% 1,8-diiodooctane), respectively, and stirred overnight on a hot plate at 50 °C. When the solutions were cooled down to room temperature, they were spin-coated on the pretreated substrates to obtain the thicknesses of ~100 nm by controlling the spinning rate. The Y6 and IT-4F based films were then annealed at 110 °C and 100 °C for 10 min, respectively, then were transferred to the vacuum chamber. At a vacuum level of 1×10^{-7} Torr, a thin layer (10 nm) of MoO_3 was then thermally deposited as the anode interlayer, followed by thermal deposition of 100 nm of Ag as the top electrode through a shadow mask. The final device structure was ITO/ZnO/C60-SAM/PM6:Y6 or PM6:IT-4F/MoO_3/Ag, and the active area of all devices were 0.08 cm^2.

Supporting Information

The supporting information for this article is available on the WWW under https://doi.org/10.1002/cjoc.202200481.

Acknowledgement

R.D. sincerely acknowledges the SPECIFIC Innovation and Knowledge Centre (EP/N020863/1) and ATIP (EP/T028513/1) grant for providing financial support. Hin-Lap Yip acknowledges the financial support by the Guangdong Major Project of Basic and Applied Basic Research (No. 2019B030302007); the Ministry of Science and Technology of China (No. 2019YFA0705900). Guichuan Zhang acknowledges the financial support by the National Natural Science Foundation of China (No. 51903095) and the Natural Science Foundation of Guangdong Province (No. 2021A1515010959).

References

[1] Tang, C. W. Two-layer organic photovoltaic cell. *Appl. Phys. Lett.* **1986**, *48*, 183–185.
[2] Bi, P.; Zhang, J.; Wang, J.; Ren, J. S. Progress in Organic Solar Cells: Materials, Physics and Device Engineering. *Chin. J. Chem.* **2021**, *39*, 2607–2625.
[3] Xu, X.; Yu, L.; Peng, Q. Recent Advances in Wide Bandgap Polymer Donors and Their Applications in Organic Solar Cells. *Chin. J. Chem*. **2021**, *39*, 243–254.
[4] Lee, J.; Cha, H.; Yao, H.; Hou, J.; Suh, Y.-H.; Jeong, S.; Lee, K.; Durrant, J. R. Toward Visibly Transparent Organic Photovoltaic Cells Based on a Near-Infrared Harvesting Bulk Heterojunction Blend. *ACS Appl. Mater. Interfaces* **2020**, *12*, 32764–32770.
[5] Han, S.; Deng, Y.; Han, W.; Ren, G.; Song, Z.; Liu, C.; Guo, W. Recent advances of semitransparent organic solar cells. *Solar Energy* **2021**, *225*, 97–107.
[6] Meitzner, R.; Schubert, U. S.; Hoppe, H. Agrivoltaics—The Perfect Fit for the Future of Organic Photovoltaics. *Adv. Energy Mater*. **2021**, *11*, 2002551.
[7] Cardinaletti, I.; Vangerven, T.; Nagels, S.; Cornelissen, R.; Schreurs, D.; Hruby, J.; Vodnik, J.; Devisscher, D.; Kesters, J.; D'Haen, J.; Franquet, A.; Spampinato, V.; Conard, T.; Maes, W.; Deferme, W.; Manca, J. v. Organic and perovskite solar cells for space applications. *Solar Energy Mater. Solar Cells* **2018**, *182*, 121–127.
[8] Ryu, H. S.; Park, S. Y.; Lee, T. H.; Kim, J. Y.; Woo, H. Y. Recent progress in indoor organic photovoltaics. *Nanoscale* **2020**, *12*, 5792–5804.
[9] Hou, X.; Wang, Y.; Lee, H. K. H.; Datt, R.; Uslar Miano, N.; Yan, D.; Li, M.; Zhu, F.; Hou, B.; Tsoi, W. C.; Li, Z. Indoor application of emerging photovoltaics—progress, challenges and perspectives. J. Mater. Chem. A Mater. **2020**, *8*, 21503–21525.
[10] Barbé, J.; Pockett, A.; Stoichkov, V.; Hughes, D.; Lee, H. K. H.; Carnie, M.; Watson, T.; Tsoi, W. C. *In situ* investigation of perovskite solar cells' efficiency and stability in a mimic stratospheric environment for high-altitude pseudo-satellites. *J. Mater. Chem. C Mater.* **2020**, *8*, 1715–1721.
[11] Kaltenbrunner, M.; White, M. S.; Głowacki, E. D.; Sekitani, T.; Someya, T.; Sariciftci, N. S.; Bauer, S. Ultrathin and lightweight organic solar cells with high flexibility. *Nat. Commun.* **2012**, *3*, 770.
[12] Verduci, R.; Romano, V.; Brunetti, G.; Yaghoobi Nia, N.; di Carlo, A.; D'Angelo, G.; Ciminelli, C. Solar Energy in Space Applications: Review and Technology Perspectives. *Adv. Energy Mater*. **2022**, *12*, 2200125.
[13] Kaltenbrunner, M.; Adam, G.; Głowacki, E. D.; Drack, M.; Schwödiauer, R.; Leonat, L.; Apaydin, D. H.; Groiss, H.; Scharber, M. C.; White, M. S.; Sariciftci, N. S.; Bauer, S. Flexible high power-per-weight perovskite solar cells with chromium oxide–metal contacts for improved stability in air. *Nat. Mater*. **2015**, *14*, 1032–1039.
[14] Lee, H. K. H.; Stewart, K.; Hughes, D.; Barbé, J.; Pockett, A.; Kilbride, R. C.; Heasman, K. C.; Wei, Z.; Watson, T. M.; Carnie, M. J.; Kim, J.-S.; Tsoi, W. C. Proton Radiation Hardness of Organic Photovoltaics: An In-Depth Study. *Solar RRL* **2022**, *6*, 2101037.
[15] Park, S.; Heo, S. W.; Lee, W.; Inoue, D.; Jiang, Z.; Yu, K.; Jinno, H.; Hashizume, D.; Sekino, M.; Yokota, T.; Fukuda, K.; Tajima, K.; Someya, T. Self-powered ultra-flexible electronics via nano-grating-patterned organic photovoltaics. *Nature* **2018**, *561*, 516–521.
[16] Zhu, L.; Zhang, M.; Xu, J.; Li, C.; Yan, J.; Zhou, G.; Zhong, W.; Hao, T.; Song, J.; Xue, X.; Zhou, Z.; Zeng, R.; Zhu, H.; Chen, C. C.; MacKenzie, R. C. I.; Zou, Y.; Nelson, J.; Zhang, Y.; Sun, Y.; Liu, F. Single-junction organic solar cells with over 19% efficiency enabled by a refined double-fibril network morphology. *Nat. Mater.* **2022**, *21*, 656–663.
[17] Zheng, Z.; Wang, J.; Bi, P.; Ren, J.; Wang, Y.; Yang, Y.; Liu, X.; Zhang, S.; Hou, J. Tandem Organic Solar Cell with 20.2% Efficiency. *Joule* **2022**, *6*, 171–184.
[18] Xie, L.; Yang, C.; Zhou, R.; Wang, Z.; Zhang, J.; Lu, K.; Wei, Z. Ternary Organic Solar Cells Based on Two Non-fullerene Acceptors with Complimentary Absorption and Balanced Crystallinity. *Chin. J. Chem.* **2020**, *38*, 935–940.
[19] Li, G.; Wu, J.; Fang, J.; Guo, X.; Zhu, L.; Liu, F.; Zhang, M.; Li, Y. A Non-Fullerene Acceptor with Chlorinated Thienyl Conjugated Side Chains for High-Performance Polymer Solar Cells via Toluene Processing. Chin. J. Chem. **2020**, *38*, 697–702.
[20] Sun, H.; Song, X.; Xie, J.; Sun, P.; Gu, P.; Liu, C.; Chen, F.; Zhang, Q.; Chen, Z.-K.; Huang, W. PDI Derivative through Fine-Tuning the Molecular Structure for Fullerene-Free Organic Solar Cells. *ACS Appl. Mater. Interfaces* **2017**, *9*, 29924–29931.
[21] Xu, Y.; Yao, H.; Hou, J. Recent Advances in Fullerene-free Polymer Solar Cells: Materials and Devices. *Chin. J. Chem*. **2019**, *37*, 207–215.
[22] Chen, W.; Zhang, Q. Recent progress in non-fullerene small molecule acceptors in organic solar cells (OSCs). *J. Mater. Chem. C Mater.* **2017**, *5*, 1275–1302.
[23] Schreurs, D.; Nagels, S.; Cardinaletti, I.; Vangerven, T.; Cornelissen, R.; Vodnik, J.; Hruby, J.; Deferme, W.; Manca, J. v. Methodology of the first combined in-flight and ex situ stability assessment of organic-based solar cells for space applications. *J. Mater. Res.* **2018**, *33*, 1841–1852.
[24] Reb, L. K.; Böhmer, M.; Predeschly, B.; Grott, S.; Weindl, C. L.; Ivandekic, G. I.; Guo, R.; Dreißigacker, C.; Gernhäuser, R.; Meyer, A.; Müller-Buschbaum, P. Perovskite and Organic Solar Cells on a Rocket Flight. *Joule* **2020**, *4*, 1880–1892
[25] Lee, H. K. H.; Durrant, J. R.; Li, Z.; Tsoi, W. C. Stability study of thermal cycling on organic solar cells. *J. Mater. Res.* **2018**, *33*, 1902–1908.
[26] Barbé, J.; Lee, H. K. H.; Toyota, H.; Hirose, K.; Sato, S.; Ohshima, T.; Heasman, K. C.; Tsoi, W. C. Characterization of stability of benchmark organic photovoltaic films after proton and electron bombardments. *Appl. Phys. Lett.* **2018**, *113*, 183301.
[27] Guo, S.; Brandt, C.; Andreev, T.; Metwalli, E.; Wang, W.; Perlich, J.; Müller-Buschbaum, P. First Step into Space: Performance and Morphological Evolution of P3HT:PCBM Bulk Heterojunction Solar Cells

under AM0 Illumination. *ACS Appl. Mater. Interfaces* **2014**, *6*, 17902–17910.
[28] Kumar, A.; Rosen, N.; Devine, R.; Yang, Y. Interface design to improve stability of polymer solar cells for potential space applications. *Energy Environ. Sci.* **2011**, *4*, 4917.
[29] Kumar, A.; Devine, R.; Mayberry, C.; Lei, B.; Li, G.; Yang, Y. Origin of Radiation-Induced Degradation in Polymer Solar Cells. *Adv. Funct. Mater.* **2010**, *20*, 2729–2736.
[30] Martynov, I. V.; Akkuratov, A. V.; Luchkin, S. Y.; Tsarev, S. A.; Babenko, S. D.; Petrov, V. G.; Stevenson, K. J.; Troshin, P. A. Impressive Radiation Stability of Organic Solar Cells Based on Fullerene Derivatives and Carbazole-Containing Conjugated Polymers. *ACS Appl. Mater. Interfaces* **2019**, *11*, 21741–21748.
[31] Zhao, W.; Li, S.; Yao, H.; Zhang, S.; Zhang, Y.; Yang, B.; Hou, J. Molecular Optimization Enables over 13% Efficiency in Organic Solar Cells. *J. Am. Chem. Soc*. **2017**, *139*, 7148–7151.
[32] Elumalai, N. K.; Uddin, A. Open circuit voltage of organic solar cells: an in-depth review. *Energy Environ. Sci.* **2016**, *9*, 391–410.
[33] Kemerink, M.; Kramer, J. M.; Gommans, H. H. P.; Janssen, R. A. J. Temperature-dependent built-in potential in organic semiconductor devices. *Appl. Phys. Lett.* **2006**, *88*, 192108.
[34] Koster, L. J. A.; Smits, E. C. P.; Mihailetchi, V. D.; Blom, P. W. M. Device model for the operation of polymer/fullerene bulk heterojunction solar cells. *Phys. Rev. B* **2005**, *72*, 085205.
[35] Riedel, I.; Parisi, J.; Dyakonov, V.; Lutsen, L.; Vanderzande, D.; Hummelen, J. C. Effect of Temperature and Illumination on the Electrical Characteristics of Polymer–Fullerene Bulk-Heterojunction Solar Cells. *Adv. Funct. Mater.* **2004**, *14*, 38–44.
[36] Chirvase, D.; Chiguvare, Z.; Knipper, M.; Parisi, J.; Dyakonov, V.; Hummelen, J. C. Temperature dependent characteristics of poly(3 hexylthiophene)-fullerene based heterojunction organic solar cells. *J. Appl. Phys.* **2003**, *93*, 3376–3383.
[37] Elumalai, N. K.; Vijila, C.; Jose, R.; Zhi Ming, K.; Saha, A.; Ramakrishna, S. Simultaneous improvements in power conversion efficiency and operational stability of polymer solar cells by interfacial engineering. *Phys. Chem. Chem. Phys*. **2013**, *15*, 19057.
[38] Gao, F.; Tress, W.; Wang, J.; Inganäs, O. Temperature Dependence of Charge Carrier Generation in Organic Photovoltaics. *Phys. Rev. Lett.* **2015**, *114*, 128701.
[39] Elumalai, N. K.; Saha, A.; Vijila, C.; Jose, R.; Jie, Z.; Ramakrishna, S. Enhancing the stability of polymer solar cells by improving the conductivity of the nanostructured MoO_3 hole-transport layer. *Phys. Chem. Chem. Phys.* **2013**, *15*, 6831.
[40] Rand, B. P.; Burk, D. P.; Forrest, S. R. Offset energies at organic semiconductor heterojunctions and their influence on the open-circuit voltage of thin-film solar cells. *Phys. Rev. B* **2007**, *75*, 115327.
[41] Kupgan, G.; Chen, X. K.; Brédas, J. L. Molecular packing of non-fullerene acceptors for organic solar cells: Distinctive local morphology in Y6 vs. ITIC derivatives. *Mater. Today Adv.* **2021**, *11*, 100154.
[42] Wang, Z.; Peng, Z.; Xiao, Z.; Seyitliyev, D.; Gundogdu, K.; Ding, L.; Ade, H. Thermodynamic Properties and Molecular Packing Explain Performance and Processing Procedures of Three D18:NFA Organic Solar Cells. *Adv. Mater*. **2020**, *32*, 2005386.
[43] Hu, X.; Datt, R.; He, Q.; Kafourou, P.; Ka Hin Lee, H.; White, A. J. P.; Tsoi, W. C.; Heeney, M. Facile synthesis of annulated benzothiadiazole derivatives and their application as medium band gap acceptors in organic photovoltaic devices. *J. Mater. Chem. C Mater.* **2022**, *10*, 9249–9256.
[44] Tang, A.; Song, W.; Xiao, B.; Guo, J.; Min, J.; Ge, Z.; Zhang, J.; Wei, Z.; Zhou, E. Benzotriazole-Based Acceptor and Donors, Coupled with Chlorination, Achieve a High V_{OC} of 1.24 V and an Efficiency of 10.5% in Fullerene-Free Organic Solar Cells. *Chem. Mater.* **2019**, *31*, 3941–3947.
[45] Park, S. Y.; Li, Y.; Kim, J.; Lee, T.; Walker, H. B.; Woo, H. Y.; Kim, J. Y. Alkoxybenzothiadiazole-Based Fullerene and Nonfullerene Polymer Solar Cells with High Shunt Resistance for Indoor Photovoltaic Applications. *ACS Appl. Mater Interfaces* **2018**, *10*, 3885–3894.
[46] Bauer, N.; Zhang, Q.; Zhao,; Ye, J. L.; Kim, J.-H.; Constantinou, I.; Yan, L.; So, F.; Ade, H.; Yan, H.; You, W. Comparing non-fullerene acceptors with fullerene in polymer solar cells: a case study with FTAZ and PyCNTAZ. *J. Mater. Chem. A Mater.* **2017**, *5*, 4886–4893.
[47] Martynov, I. v.; Akkuratov, A.; Troshin, P. A.; Visoly-Fisher, I.; Katz, E. A. Naphthalene dithiol additive reduces trap-assisted recombination and improves outdoor operational stability of organic solar cells. *Sustain. Energy Fuels* **2022**, *6*, 2727–2733.
[48] Liu, C.; Tu, J.; Hu, X.; Huang, Z.; Meng, X.; Yang, J.; Duan, X.; Tan, L.; Li, Z.; Chen, Y. Enhanced Hole Transportation for Inverted Tin-Based Perovskite Solar Cells with High Performance and Stability. Adv. Funct. Mater. **2019**, *29*, 1808059.
[49] Wu, J.; Luke, J.; Lee, H. K. H.; Shakya Tuladhar, P.; Cha, H.; Jang, S.-Y.; Tsoi, W. C.; Heeney, M.; Kang, H.; Lee, K.; Kirchartz, T.; Kim, J.-S.; Durrant, J. R. Tail state limited photocurrent collection of thick photoactive layers in organic solar cells. *Nat. Commun*. **2019**, *10*, 5159.
[50] McMillon-Brown, L.; Crowley, K. M.; VanSant, K. T.; Peshek, T. J. Prospects for Perovskites in Space. In *2021 IEEE 48th Photovoltaic Specialists Conference* (*PVSC*), IEEE, **2021**, pp. 0222–0225.

Manuscript received: July 30, 2022
Manuscript revised: September 1, 2022
Manuscript accepted: September 5, 2022
Accepted manuscript online: September 8, 2022
Version of record online: XXXX, 2022

The Authors

Left to Right: Ram Datt, Harrison Ka Hin Lee, Guichuan Zhang, Hin-Lap Yip, Wing Chung Tsoi

